Identification of p58^{IPK} as a Novel Neuroprotective Factor for Retinal Neurons

Evgenii Boriushkin,[1,2] Joshua J. Wang,[1–3] Junhua Li,[1,2] Guangjun Jing,[3] Gail M. Seigel,[2,4] and Sarah X. Zhang[1–3]

[1]Department of Ophthalmology and Biochemistry/Ross Eye Institute, University at Buffalo/SUNY, Buffalo, New York, United States
[2]SUNY Eye Institute, State University of New York, Buffalo, New York, United States
[3]Department of Medicine, University of Oklahoma Health Sciences Center, Oklahoma City, Oklahoma, United States
[4]Center for Hearing & Deafness, University at Buffalo, Buffalo/SUNY, New York, United States

Correspondence: Sarah X. Zhang, Department of Ophthalmology/Ross Eye Institute, University at Buffalo, State University of New York, 3435 Main Street, Buffalo, NY 14214, USA; xzhang38@buffalo.edu.

Submitted: July 9, 2014
Accepted: January 25, 2015

Citation: Boriushkin E, Wang JJ, Li J, Jing G, Seigel GM, Zhang SX. Identification of p58^{IPK} as a novel neuroprotective factor for retinal neurons. *Invest Ophthalmol Vis Sci.* 2015;56:1374–1386. DOI:10.1167/iovs.14-15196

Purpose. Endoplasmic reticulum (ER)-resident chaperone protein p58^{IPK} plays a vital role in regulation of protein folding and biosynthesis. The goal of this study was to examine the role of p58^{IPK} in retinal neuronal cells under normal and stressed conditions.

Methods. Retinal expression of p58^{IPK}, retinal morphology, apoptosis, ER stress, and apoptotic gene expression were examined in p58^{IPK} knockout (KO) and/or wild-type (WT) mice with or without intravitreal injection of N-methyl-D-aspartic acid (NMDA). In in vitro experiments, differentiated R28 retinal neuronal cells transduced with adenovirus encoding p58^{IPK} (Ad-p58^{IPK}) or control virus (Ad-LacZ) were exposed to tunicamycin (TM) or hydrogen peroxide (H_2O_2). Levels of ER stress, apoptosis, and cell survival were evaluated.

Results. Chaperone protein p58^{IPK} is expressed predominantly in retinal ganglion cells (RGC), inner retinal neurons, and the photoreceptor inner segments. Mice lacking p58^{IPK} exhibited increased CHOP expression and loss of RGCs with aging (8–10 months). Intravitreal injection of NMDA induced retinal ER stress and increased p58^{IPK} expression in WT mice; this resulted in greater ER stress and enhanced RGC apoptosis in p58^{IPK} KO mice. In cultured R28 cells, overexpression of p58^{IPK} significantly reduced eIF2α phosphorylation, decreased CHOP expression, and alleviated the activation of caspase-3 and PARP. Overexpression of p58^{IPK} also protected against oxidative and ER stress-induced cell apoptosis. Furthermore, p58^{IPK} downregulated the proapoptotic gene Bax and upregulated the antiapoptotic gene Bcl-2 expression in stressed R28 cells.

Conclusions. Our study has demonstrated a protective role of p58^{IPK} in retinal neurons, which may act in part through a mechanism involving modulation of ER homeostasis and apoptosis, particularly under conditions of cellular stresses.

Keywords: p58^{IPK}, chaperone, endoplasmic reticulum stress, neuronal cells

Protein homeostasis is essential for cell survival. Disturbed protein homeostasis in the endoplasmic reticulum (ER) is known as ER stress.[1] Many factors, such as hypoxia, viral and bacterial infections, inhibition of protein glycosylation, and disturbance of calcium levels can cause ER stress. In order to restore homeostasis in the ER, eukaryotic cells have developed an unfolded protein response (UPR) to facilitate protein folding through enhanced expression/activity of ER chaperones while reducing new protein influx into the ER lumen.[2] Endoplasmic reticulum chaperones recognize and bind misfolded proteins, promoting their refolding and preventing dangerous nonspecific interactions or aggregation of misfolded proteins. Protein p58^{IPK} is an ER chaperone belonging to the heat shock protein 40 kDa (Hsp40) family.[3–5] It promotes protein folding in the ER in association with another ER chaperone named glucose-regulated protein 78 kDa (GRP78)[6] and is essential for maintaining the homeostatic environment of the ER.[7–9] Apart from participating in protein folding in the ER lumen, p58^{IPK} is also present in the cytoplasm and acts as an inhibitor of eIF2 kinases, or RNA-activated protein kinase (PKR).[10–12] By inhibiting PKR, p58^{IPK} modulates protein synthesis and regulates inflammatory response.[10–12]

Endoplasmic reticulum chaperones play important roles in guarding the fidelity of protein folding, especially in those cells with vigorous metabolism. Retinal neuronal cells are very metabolically active and highly vulnerable to cellular disturbances. Many ocular disorders such as glaucoma,[13] optic neuropathies,[14] and retinal vascular diseases[15] cause ER stress in retinal neurons. Prolonged or unimpeded ER stress in these cells can lead to apoptosis.[16] Aside from ER stress, oxidative stress can also trigger the death of retinal neuronal cells.[17] Glutamate, an excitatory neurotransmitter in the central nervous system and in the eye, has been shown to induce neuronal cell death through activation of the N-methyl-D-aspartate (NMDA)-type glutamate receptor.[18] Excessive activation of NMDA receptors results in calcium burst in cytosol from the ER and extracellular space.[19,20] Intracellular Ca^{2+} overload results in increased production of nitric oxide, disturbance of the redox system and induces oxidative stress. It also leads to ER dysfunction and subsequent accumulation of misfolded

proteins and ER stress, which contributes to cell death in the neural retina.[21]

In the present study, we examined the role of p58IPK in retinal neuronal cells using in vivo and in vitro models. We demonstrated that p58IPK was highly expressed in retinal ganglion cells (RGCs) and inner retinal neurons of wild-type (WT) mice. Knockout (KO) p58IPK mice demonstrated a reduced number of RGCs and were more sensitive to NMDA-induced retinal neuronal cell death compared with WT mice. Our in vitro experiments showed that endogenous and exogenous p58IPK was localized in the ER in stressed conditions and overexpression of p58IPK could protect differentiated R28 cells from ER stress and oxidative stress-induced cell injury and apoptosis.

Materials and Methods

Materials

Laminin, N-methyl D-aspartate (NMDA), and tunicamycin (TM) were purchased from Sigma-Aldrich Laboratories (St. Louis, MO, USA). Fetal bovine serum, Dulbecco's modified Eagle's medium (DMEM), 1 × MEM on-essential amino acids, 1 × MEM vitamins, and sodium bicarbonate were obtained from Gibco Laboratories (Grand Island, NY, USA). Phenylephrine hydrochloride and tropicamide were obtained from Bausch and Lomb (Tampa, FL, USA). Radioimmunoprecipitation buffer, inhibitor mixture, PMSF, sodium orthovanadate were purchase from Santa Cruz Biotechnology (Dallas, TX, USA). Mounting medium with DAPI was from Vector Laboratories, Inc. (VECTASHIELD; Burlingame, CA, USA).

Mice

Knockout p58IPK mice were provided by Michael G. Katze (University of Washington, Seattle, WA, USA). All experimental procedures were performed in compliance with animal protocols approved by the Institutional Animal Care and Use Committees at the State University of New York at Buffalo and University of Oklahoma Health Sciences Center. Intravitreal injection of NMDA was performed under a surgical microscope as described in our previous study.[22] We injected 20 nmol of NMDA in 2 μL of sterilized PBS was injected into the one eye and equal amount of PBS into the contralateral eye as control. Mice were killed 8 hours after injection.

Cell Culture

The immortalized R28 rat retinal cell line has been used for a variety of in vitro studies as a model of retinal neuronal behavior and function for over 20 years (reviewed in Seigel[23]). For our studies, R28 cells were grown in Dulbecco's modified Eagle's medium (DMEM) with 5.5 mM glucose, 10% newborn calf serum, 1 × MEM nonessential amino acids, 1 × MEM vitamins, 0.37% sodium bicarbonate, 0.058% L-glutamine, and 80 μg/mL gentamicin. The cells were differentiated into neurons on laminin-coated plates or coverslips with addition of 25 μM cell-permeable cAMP as described previously.[24] Confluent cells were quiescent for 12 h in DMEM containing 1% FBS followed by the desired treatments.

Construction and Transduction of Adenoviruses

Recombinant adenovirus expressing murine P58IPK was generated using the AdEasy system (Agilent Technologies, Santa Clara, CA, USA) according to the manufacturer's instructions. Briefly, full length of murine P58IPK gene was cloned and inserted into the BgI II-XhoI sites of the pShuttle-CMV vector. Primer pairs used for cloning p58IPK were as following: Forward GAAGAT CTGCCACCATGGTGGCCCCCGGCTCG, Reverse CCGCTC GAGTTAATTGAAGTGGAACTTAAATC. The linearized shuttle vector Pme I was then coelectroporated with pAdEasy-1 into BJ5183 *E. coli* cells and the recombinant adenoviral plasmid was transfected into the packing 293AD cells to generate recombinant adenoviruses. Large-scale preparation of adenoviruses was completed by repeatedly transduction of 293AD cells. To overexpress P58IPK, R28 cells at 70% confluence were transduced with adenoviruses encoding p58IPK (Ad-p58IPK) at a multiplicity of infection (MOI) of 25 and 50 for 24 hours. Adenovirus expressing LacZ (Ad-LacZ) of the same MOIs was used as a control.

Immunoblotting

Retinas and cells were lysed and sonicated in radioimmunoprecipitation buffer with protease inhibitor mixture, PMSF, and sodium orthovanadate. The total amount of protein was determined by protein assay (Thermo Fisher Scientific, Inc., Rockford, IL, USA). The samples were resolved by SDS-PAGE and blotted with specific antibodies: anti-p58IPK, anti-CHOP, anti-p-eIF2α; anti-Poly (ADP-ribose) polymerase (PARP); anti-cleaved caspase-3 (Cell Signaling Technology, Boston, MA, USA); and anti-KDEL (Abcam, Cambridge, MA, USA). The same membrane was blotted with an anti-β-actin antibody (Santa Cruz Biotechnology) as a loading control.

Quantitative Real-Time PCR

Total RNA was extracted from R28 cells using an RNeasy Mini Kit (Qiagen, Valencia, CA, USA) and cDNA was synthesized using a high-capacity cDNA Reverse Transcription kit (Applied Biosystems, Foster City, CA, USA) as described previously.[25] Quantitative real-time PCR was performed on PCR System (Bio-Rad Real-Time; Bio-Rad Laboratories, Hercules, CA, USA) using the following primers: Bcl-2: forward 5′-CGA CTT TGC AGA GAT GTC CA-3′, reverse 5′-ATG CCG GTT CAG GTA CTC AG-3′; Bax: forward 5′-GTG GTT GCC CTC TTC TAC TTT G-3′, reverse 5′-CAC AAA GAT GGT CAC TGT CTG C-3.′ Data were analyzed by the comparative threshold cycle method using 18s ribosomal RNA (forward 5′-GGG AGG TAG TGA CGA AAA ATA ACA AT-3′; reverse 5′-TTG CCC TCC AAT GGA TCC T-3′) as an internal control.

Immunofluorescence Staining

Transverse, 10-μm thick cryostat sections of mouse eyes were incubated for 60 minutes in PBS containing 10% normal goat serum to block nonspecific binding. Sections were then incubated with primary antibodies against p58IPK (1:100; Abcam, Cambridge, MA, USA), CHOP (1:100), Brn3a (1:100; Millipore, Corp., Temecula, CA, USA), and GFAP (1:100; Dako, Glostrup, Denmark) overnight at 4°C. After washing, the sections were incubated with Texas Red-conjugated secondary antibody (1:500) and mounted with mounting medium with DAPI (Vector Laboratories, Inc.). For immunofluorescence staining of R28 cells, cells were incubated with antibodies against p58IPK (1:100) and KDEL (1:100) overnight at 4°C and then incubated with Alexa Fluor 488 goat anti-rabbit (1:500) and Cy3 goat anti-mouse (1:500) antibodies (Invitrogen, Eugene, OR, USA). The retinal sections and cells were observed under a laser confocal microscope (LSM 510; Carl Zeiss Microscopy, Jena, Germany).

Counting Ganglion Cells in Retinal Flat Mounts

Retinas were dissected as flattened whole mounts, permeabilized in PBS with 0.5% Triton X-100, and blocked with 10%

Investigative Ophthalmology & Visual Science

normal goat serum. Then, the retinas were incubated for 3-5 days at 4°C with goat-antiBrn3a (c-20) antibody (1:100; Santa Cruz Biotechnology, Inc.). After washing, the retinas were incubated for overnight with secondary antibody and mounted with the vitreous side up on slides. The retinas were observed under a microscope (Olympus BX53; Olympus Corp., [City], Japan). To count RGCs, four images with an area of 0.344 mm^2, one image per quadrant, were taken in the midperipheral retina (1200 μm of the retinal radius from the ON head) from each mouse. The numbers of RGCs were counted manually by two investigators in a masked manner and normalized per square millimeter, and an average of RGC density was acquired for each mouse and used for statistical analysis.

MTT Cell Viability Assay

After viral transduction and desired treatment, viability of R28 cells was measured with a 3-[4,5-yl]-2,5-diphenyltetrazolium bromide (MTT) assay kit (Trevigen, Gaithersburg, MD, USA) following manufacturer's instructions. Briefly, 10 μL MTT solution was added to the cells in 100 μL medium. After an incubation period of 4 hours, 100 μL detergent reagent was added and cells were incubated at 37°C for 4 hours. Absorbance was measured at 570 nm in a microplate reader.

TUNEL Assay

The terminal deoxynucleotidyl transferase-mediated dUTP nick end labeling (TUNEL) assay was done with an in situ cell death detection kit (Roche, Mannheim, Germany) as described previously.[25] As a negative control of the TUNEL reaction, a mixture without terminal transferase was used. Nuclei were stained with DAPI and TUNEL-positive cell counts were calculated as percentages of total cell number.

Histology and Morphometric Analysis

Paraffin sections of mouse eyeballs were cut along the vertical meridian through the optic nerve head. Sections were dewaxed, rehydrated, and stained with hematoxylin and eosin. The inner nuclear layer (INL) and outer nuclear layer (ONL) thicknesses were measured under light microscopy. Measurements were taken every 240 μm from the optic nerve head to the peripheral retina on both the superior and inferior portions of the retina.

Statistical Analysis

Quantitative data were expressed as mean (± SD). Statistical analyses were performed using unpaired Student's *t*-test when comparing two groups and one-way ANOVA test for three groups and more. Statistical differences were considered significant at a P value less than 0.05.

Results

Expression of p58IPK in Normal Mouse Retina

Immunostaining of retinal cryosections from WT mice shows high expression of p58IPK in the ganglion cell layer (GCL) and INL of the retina and in the inner segments of photoreceptors (Fig. 1A). In contrast, retinas from p58IPK KO mice did not show any signal of p58IPK (Fig. 1B). Interestingly, we found that in WT mice the cells in the GCL do not seem to equally express p58IPK. To determine which cell types in the GCL express p58IPK, we stained the retinal sections for brain-specific homeobox/POU domain protein 3A (Brn3a) and glial fibrillary acidic protein (GFAP), markers of RGCs[26] and astrocytes,[27] respectively. We found that Brn3a-positive RGCs are highly immunoreactive for p58IPK, while Brn3a-negative cells in the GCL show only weak staining (arrows, Fig. 1C). Consistently, astrocytes that are positive for GFAP demonstrate low immunoreactivity for p58IPK (arrow, Fig. 1D). These observations suggest a potential role of p58IPK in retinal neurons.

Knockout of p58IPK Results in CHOP-Mediated Apoptosis of RGCs

Since p58IPK functions primarily as an ER chaperone,[28] we evaluated the levels of ER stress and apoptosis of retinal cells in the p58IPK KO mice. In the retinas from p58IPK KO mice, expression of CHOP, the major proapoptotic protein induced by ER stress, was significantly increased; however, caspase-3 was not activated (Fig. 2A). Interestingly, knockout one allele of p58IPK resulted in higher retinal CHOP expression than the complete knockout. Immunostaining of retinal sections from p58IPK KO mice shows that expression of CHOP was increased in the GCL (Fig. 2B). No abnormality in retinal morphology was observed in p58IPK KO mice. Retinal morphometric analysis shows no difference in the thicknesses of INL and ONL in retinas from 8- to 10-month-old p58IPK KO and WT mice (Fig. 2C). However, p58IPK KO mice had fewer cells in the GCL compared with WT mice (Fig. 2C). To quantify the loss of ganglion cells, we performed immunostaining for Brn3a on retinal whole mounts and observed a more than 20% decrease in the number of RGCs in p58IPK KO mice compared with WT mice (Fig. 2D). These results indicated that deficiency of p58IPK, which is highly expressed in RGCs, resulted in loss of ganglion cells.

Knockout of p58IPK Exacerbates NMDA-Induced Apoptosis of Retinal Neuronal Cells

To determine whether p58IPK is involved in regulation of ER stress and cell death in retinal neurons, we examined retinal ER stress and apoptotic markers in KO and WT mice at 8 hours after intravitreal injection of NMDA. As shown in Figure 3A, intravitreal injection of NMDA at 20 nmol/eye significantly increased expression of phosphorylated eIF2α (p-eIF2α), CHOP and cleaved caspase-3 in both WT and p58IPK KO mice. However, the differences between NMDA-treated and -untreated eyes were more profound in p58IPK KO mice compared with WT controls. Furthermore, there was intense immunofluorescence of CHOP in the GCL of NMDA-treated retina (Fig. 3B) and there were more CHOP-positive cells in retinas from p58IPK KO mice (Fig. 3C). Using the TUNEL assay, we examined retinal cell apoptosis induced by NMDA in WT and p58IPK KO mice. Treatment with NMDA resulted in apoptosis of inner retinal neurons as shown by TUNEL-positive cells in the GCL and INL (Fig. 3D). These results were consistent with previous findings that NMDA could induce retinal neuronal cell death.[21,29] Quantification of the TUNEL-positive cells demonstrated that p58IPK KO mice had more apoptotic cells in the GCL compared with WT mice (Fig. 3E), suggesting that deletion of p58IPK renders retinal neuronal cells more prone to NMDA-induced ER stress and apoptosis.

Subcellular Localization of p58IPK in Normal and Stressed R28 Cells In Vitro

To further examine the role of p58IPK in protection of retinal neurons and explore the underlying mechanism, we employed immortalized R28 rat retinal cell line as an in vitro model of ER stress under controlled cell culture conditions. We chose R28 cells due to their retinal origin, predictable and controllable

Investigative Ophthalmology & Visual Science

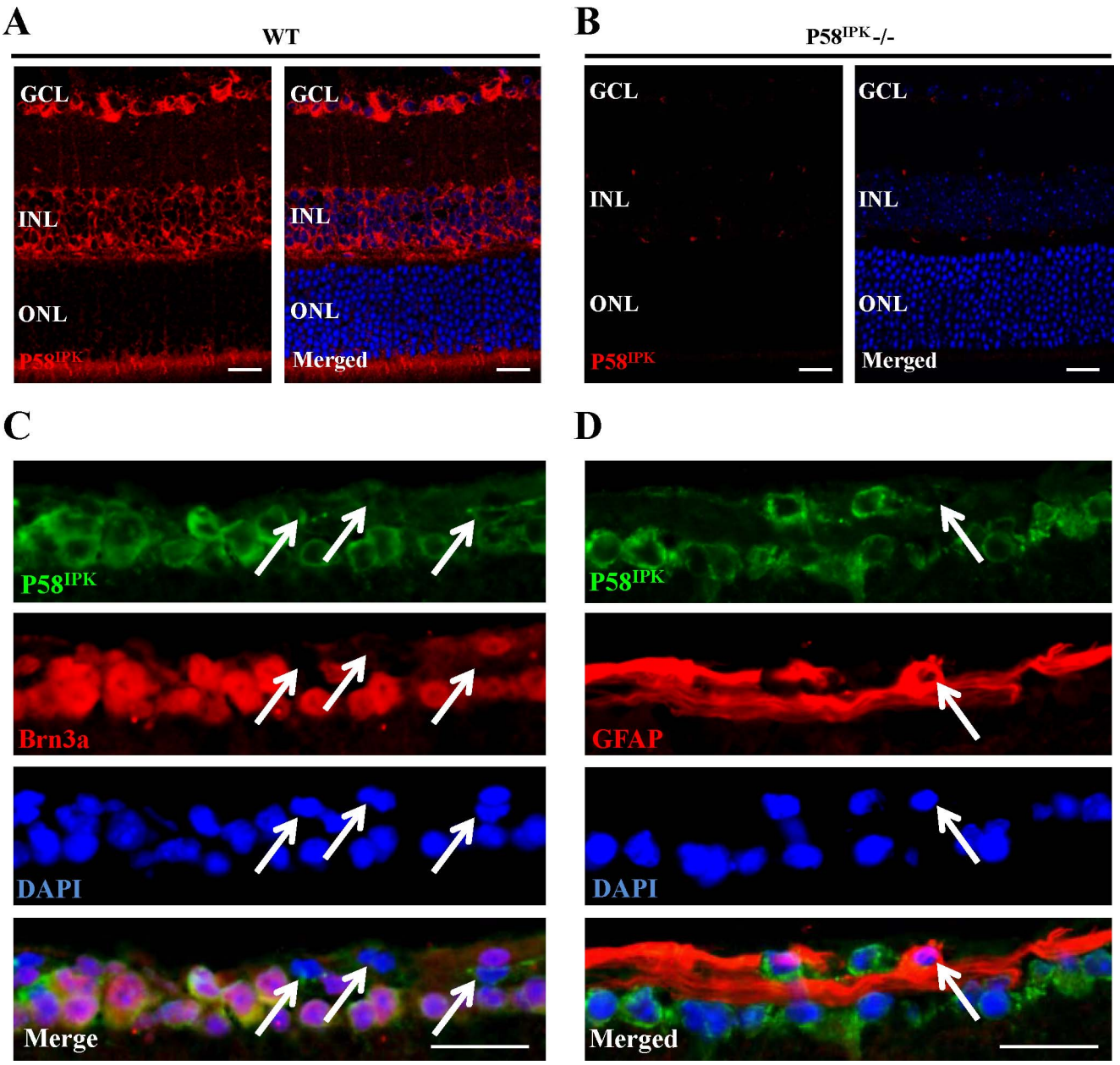

Figure 1. Protein p58IPK is highly expressed in RGCs in mice. (**A**). Immunostaining shows immunoreactivity of p58IPK in the retinal GCL, INL, and the inner segments of photoreceptors in the ONL in WT mice. Staining for p58IPK is shown in *red* and nuclei are stained in *blue* with DAPI. (**B**) Immunostaining for p58IPK in retinal sections from p58IPK KO mice. Nuclei are stained in *blue* with DAPI. (**C**) Representative images show that Brn3a (*red*)-positive ganglion cells exhibit high levels of p58IPK (*green*) in the GCL of WT mouse retina. *White arrows* indicate low p58IPK immunoreactivity in Brn3a-negative cells in GCL. Nuclei stained in *blue* with DAPI. (**D**). Representative images show that GFAP (*red*)-positive astrocytes demonstrate low levels of p58IPK (*white arrows*) compared with ganglion cells in GCL. Nuclei are stained in *blue* with DAPI. All results represent at least three mice in each group. *Scale bar*: 20 μm.

stress response, and their expression of our genes of interest. To identify the subcellular localization of p58IPK under normal and ER stress conditions, we performed immunostaining of R28 cells using anti-KDEL antibody that labels GRP78 and GRP94 as a marker for the ER. In unstressed R28 cells, the levels of p58IPK and ER-resident chaperones were low and p58IPK mostly colocalized with KDEL; however, cytosolic p58IPK was also detected (Fig. 4). Treatment with tunicamycin or overexpression of p58IPK markedly increased the intracellular levels of p58IPK, which was predominantly localized in the ER. These results suggest that p58IPK is an ER-anchored protein during ER stress.

Overexpression of p58IPK Reduces ER Stress and Apoptosis in R28 Cells In Vitro

In order to examine the role of p58IPK on ER stress and apoptosis of retinal neurons, R28 cells were treated with tunicamycin (0.1–5.0 μg/mL). Protein expression of ER chaperones, ER stress markers, and apoptotic proteins was determined by immunoblotting after 24 hours of treatment. As shown in Figure 5A, tunicamycin increased expression of p58IPK, GRP78 and GRP94, CHOP, and p-eIF2α, and triggered the cleavage of caspase-3 in a dose-dependent manner. Overexpression of p58IPK markedly decreased levels of p-

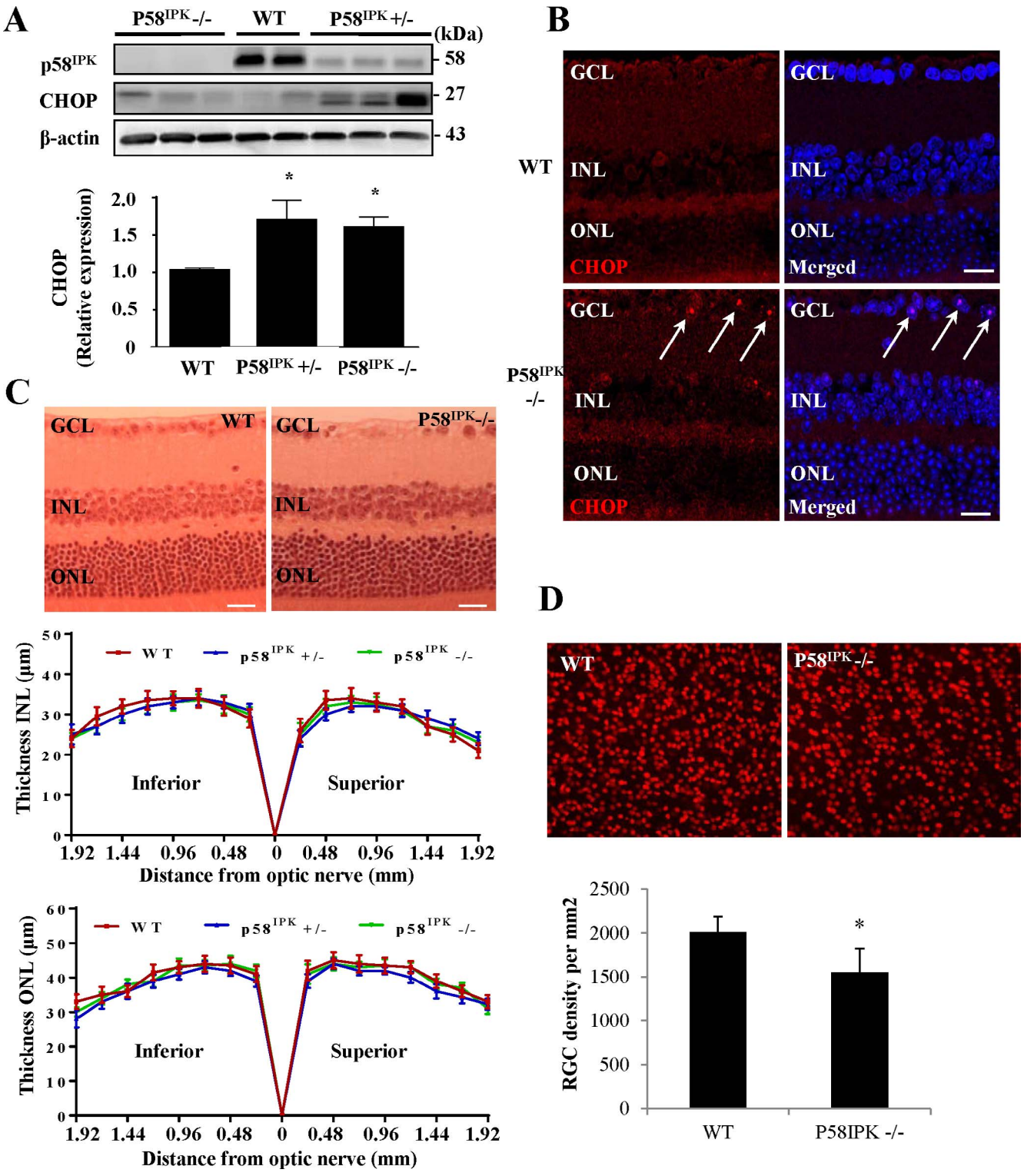

Figure 2. Loss of RGCs and increased CHOP expression in p58^{IPK} KO mice. (**A**) Immunoblotting of CHOP and p58^{IPK} in retinas from homozygous (p58$^{IPK-/-}$) and heterozygous (p58^{IPK} ±) p58^{IPK} KO and WT mice. Protein levels of CHOP were quantified by densitometry (means ± SD, $n = 4$). *$P < 0.05$ versus WT mice. (**B**) Immunostaining of CHOP (*red*) in retinas from WT and p58$^{IPK-/-}$ mice. Nuclei were stained in *blue* with DAPI. *Left panels*: CHOP staining (*red*). *Right panels*: Merged images of CHOP (*red*) with DAPI (*blue*) staining. *White arrows* indicate increased expression of CHOP in ganglion cells. Results represent at least three mice in each group. (**C**) *Upper panel*: Representative images of retinal sections (1.0 mm from the optic nerve) from 8- to 10-month-old female WT and p58$^{IPK-/-}$ mice stained with hematoxylin-eosin. *Lower panels*: Quantification of INL and ONL thickness. Data are expressed as means ± SD, $n = 6$. (**D**) *Upper panel*: Representative images of fluorescent microphotographs of flat-mounted retinas from 8- to 10-month-old female WT and p58$^{IPK-/-}$ mice. Retinal ganglion cells are shown by their immunoreactivity of Brn3a in *red*. *Lower panel*: Quantification of the number of retinal ganglion cells. Data are expressed as means ± SD, $n = 4$. *$P < 0.05$ versus WT mice.

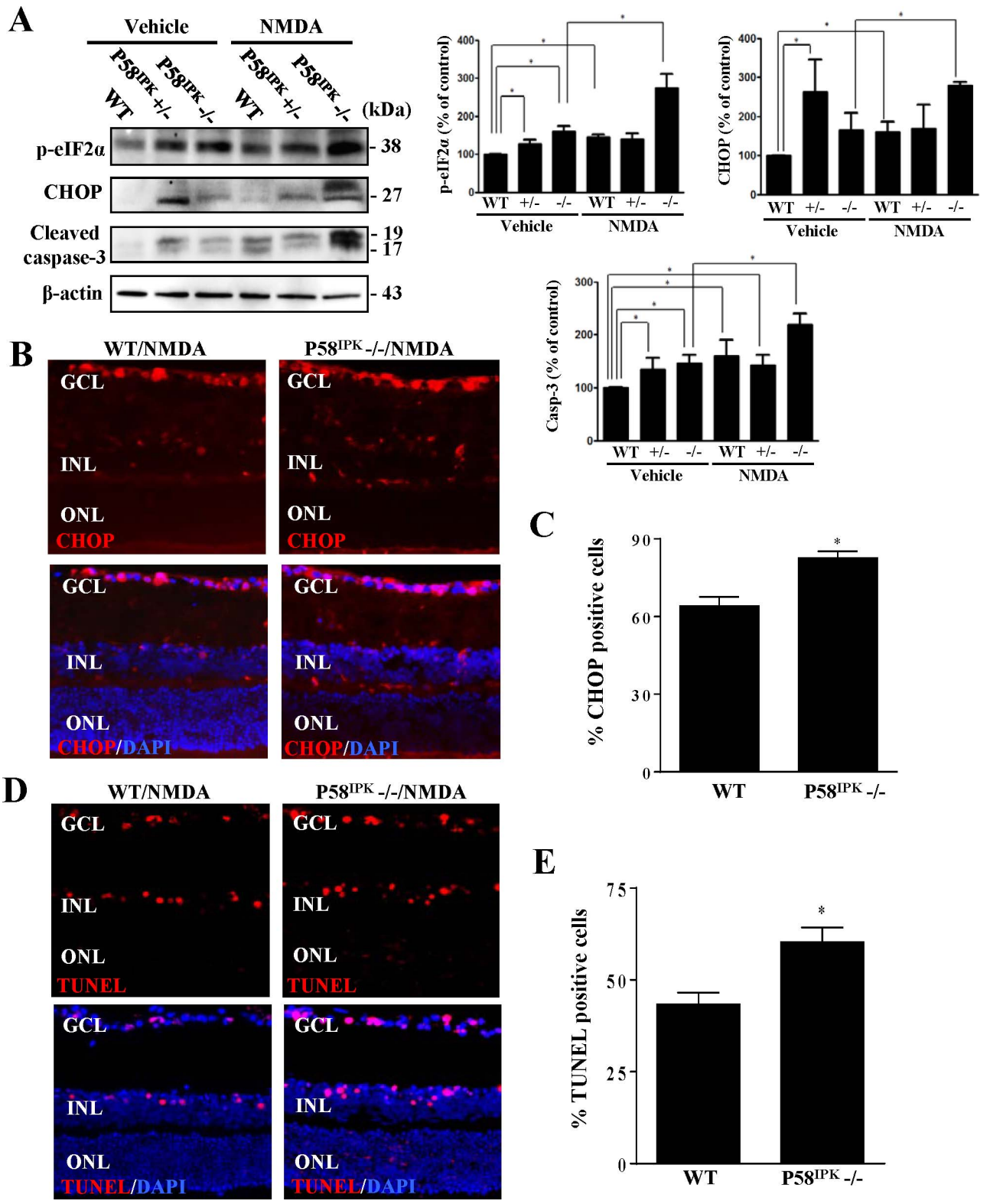

FIGURE 3. Deletion of p58IPK increases phosphorylation of eIF2α, CHOP expression and ganglion cell apoptosis after NMDA treatment. Four-month-old female WT and p58IPK–/– mice received an intravitreal injection of NMDA (20 nmol/eye) in one eye and vehicle in the contralateral eye. (**A**) Immunoblotting of protein extract from retinas after 8 hours postinjection show increased phosphorylation of eIF2α, expression of CHOP and activation of caspase-3 in p58IPK–/– compared with WT mice. Protein levels of p-eIF2α, CHOP, and cleaved caspase-3 were quantified by densitometry (means ± SD, $n = 4$). *$P < 0.01$. (**B**). Representative images of immunostaining of mouse retina for CHOP (red) in WT and p58IPK–/– mice after NMDA treatment. Nuclei were stained *blue* with DAPI. *Upper panels*: CHOP staining (*red*). *Lower panels*: Merged images of CHOP (*red*) and DAPI (*blue*) staining. (**C**) Quantification of the number of CHOP positive cells in GCL in retinal sections from 4 p58IPK–/– and 4 WT mice. Data are means ± SD. *$P < 0.01$ versus WT mice. (**D**) Representative images of TUNEL staining of mouse retina in p58IPK–/– and WT mice. *Upper panels*: TUNEL staining (*red*). *Lower panels*: merged images of TUNEL (*red*) and DAPI (*blue*) staining. (**E**) Quantification of the number of total and TUNEL positive cells in GCL in retinal sections from 4 p58IPK–/– and four WT mice. Data are expressed as means ± SD. *$P < 0.01$ versus WT mice.

Investigative Ophthalmology & Visual Science

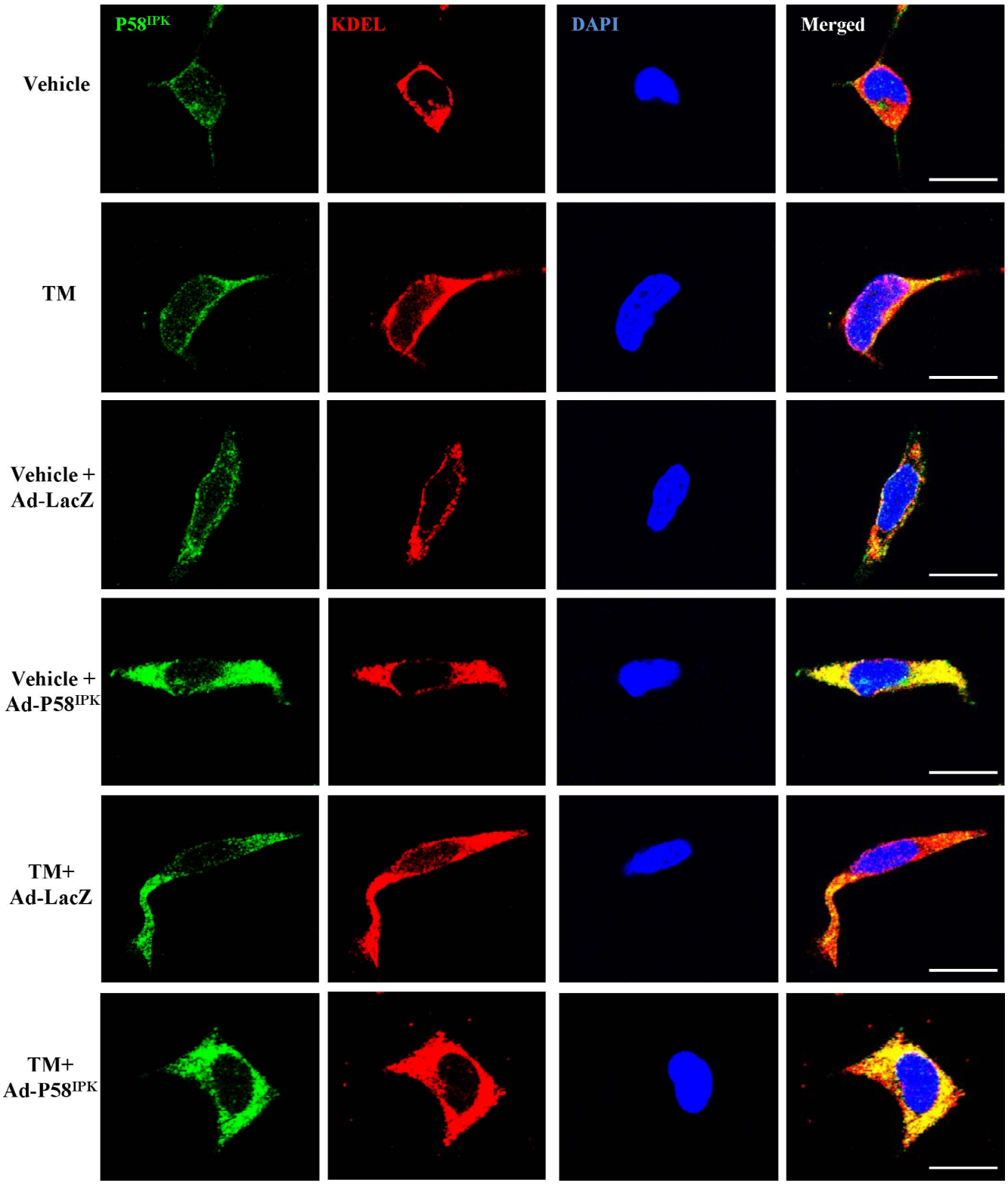

Figure 4. Protein p58IPK primarily localizes in the ER in R28 cells. Representative images show expression and localization of p58IPK (*green*) in R28 cells. We used KDEL (*red*) as a marker of the ER and nuclei were stained by DAPI in *blue*. After treatment with TM, expression of p58IPK increased and colocalized with KDEL. After viral transduction, exogenous p58IPK also colocalized with KDEL in the vehicle and TM-treated cells. *Scale bar*: 20 μm.

Investigative Ophthalmology & Visual Science

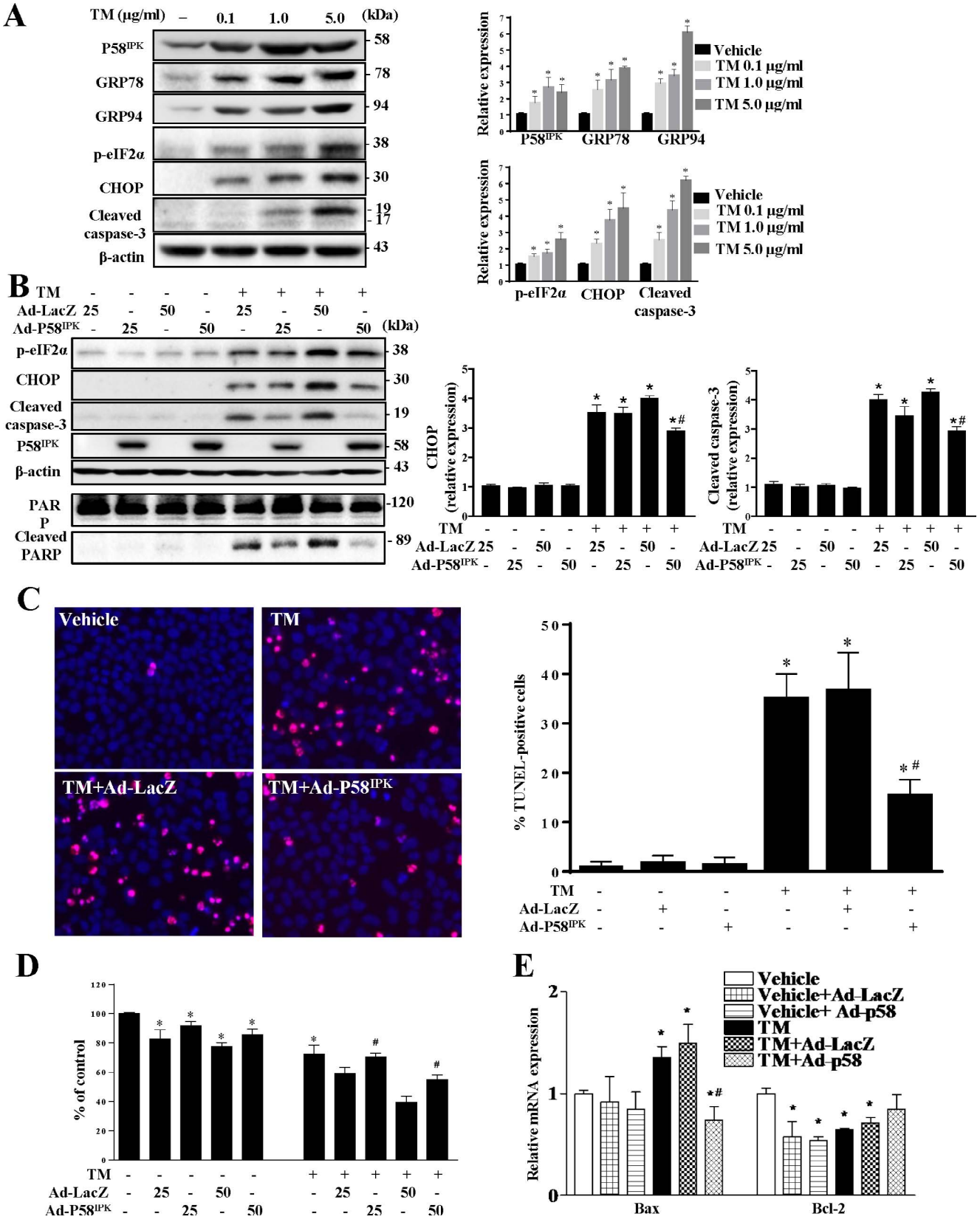

Figure 5. Overexpression of p58IPK reduces ER stress and apoptosis in R28 cells after treatment with TM. (**A**) We treated R28 cells with 0.1 to 5 μg/mL of tunicamycin (TM) for 24 hours. *Left panel*: Immunoblots showing increased expression of GRP78, GRP94, CHOP, phosphorylation of eIF2α and activation of caspase-3 in a dose-dependent manner. *Right panels*: quantification of protein expression by densitometry (means ± SD, $n = 4$). *$P < 0.001$ versus vehicle. (**B**) R28 cells were transduced with 25 or 50 MOI of adenovirus for 24 hours, followed by treatment with 1.0 μg/mL TM for an additional 24 hours. Expression of ER stress markers and apoptotic proteins was determined by immunoblotting. *Left panel*: Shows representative images of blots. *Right panels*: Show the quantification results by densitometry (means ± SD, $n = 4$). *$P < 0.001$ versus corresponding

vehicle control. #$P < 0.05$ versus corresponding Ad-LacZ group with TM treatment. (**C**) R28 cells transduced with 50 MOI of Ad-p58IPK or Ad-LacZ were treated with 1.0 μg/mL TM for 24 hours. *Left panels*: Representative images of TUNEL staining. TUNEL-positive nuclei of cells are *pink* (colocalization of TUNEL, *red* staining, with nuclear staining, *blue* with DAPI). *Right panel*: Quantification of TUNEL-positive cells in 6 to 9 frames/group. Results were expressed as means ± SD from four independent experiments. *$P < 0.001$ versus to vehicle without adenovirus. #$P < 0.01$ versus Ad-LacZ + TM. (**D**) Cell viability measured by MTT assay. Results are means ± SD of four independent experiments. *$P < 0.001$ versus vehicle without adenovirus, #$P < 0.05$ versus the corresponding Ad-LacZ group with TM treatment. (**E**) Results of qRT-PCR showing relative gene expression levels for Bax and Bcl-2. Results are means ± SD of four independent experiments. *$P < 0.01$ versus vehicle without adenovirus, #$P < 0.05$ versus Ad-LacZ + TM.

eIF2α, CHOP, and cleaved caspase-3, suggesting that overexpression of p58IPK suppresses ER stress (Fig. 5B). Next, we determined the effect of p58IPK on ER stress-mediated apoptosis using the TUNEL assay (Fig. 5C). Overexpression of p58IPK significantly reduced the percentage of TUNEL-positive cells after tunicamycin treatment compared with Ad-LacZ group. In line with these results, overexpression of p58IPK increased cell viability before and after tunicamycin treatment compared with Ad-LacZ control group (Fig. 5D). These data suggest that R28 cells are sensitive to ER stress, while overexpression of p58IPK suppresses ER stress and alleviates ER stress-induced apoptosis in R28 cells.

Protein family Bcl-2, including proapoptotic and antiapoptotic members, are master regulators of mitochondria-mediated apoptotic pathways. To determine whether overexpression of p58IPK alters the gene expression of Bcl-2 proteins in apoptotic R28 cells, we measured the mRNA level of proapoptotic protein Bax and antiapoptotic protein Bcl-2 by qRT-PCR (Fig. 5E). Compared with vehicle control, adenoviral transduction reduced the Bcl-2 level but had no effect on Bax expression. tunicamycin treatment caused a significant increase in Bax expression, which was completely abolished in cells pretreated with Ad-p58IPK. Interestingly, there was no significant difference in Bcl-2 expression in Ad-p58IPK- and Ad-LacZ-transduced cells. These results suggest that overexpression of p58IPK decreases pro-apoptotic gene Bax expression; however, it remains elusive in future studies whether reducing Bax expression contributes to the protective effect of p58IPK against apoptosis.

Overexpression of p58IPK Attenuates Oxidative Stress-Induced ER Stress and Apoptosis in R28 Cells

To induce oxidative stress, R28 cells were treated with 100 to 500 μM of hydrogen peroxide (H_2O_2) for 8 hours and protein expression was determined by immunoblotting. As shown in Figure 6A, treatment with H_2O_2 significantly increased expression of GRP78, GRP94, CHOP, p-eIF2α, and cleaved caspase-3, but did not alter the expression of p58IPK. Overexpression of p58IPK decreased levels of p-eIF2α, CHOP and cleaved caspase-3 compared with the Ad-LacZ group (Fig. 6B). In addition, overexpression of p58IPK significantly reduced the percentage of TUNEL-positive R28 cells after treatment with H_2O_2 compared with the Ad-LacZ group (Fig. 6C). As shown in Figure 6D, overexpression of p58IPK increased cell viability before and after H_2O_2 treatment compared with Ad-LacZ control group. These results indicate that overexpression of p58IPK significantly enhances the resistance of R28 cells to oxidative stress-induced ER stress and apoptosis. Similarly, we measured the expression of Bax and Bcl-2 in cells after H_2O_2 treatment (Fig. 6E). We found that overexpression of p58IPK significantly reduced Bax expression induced by H_2O_2 but increased Bcl-2 expression compared with the Ad-LacZ group. These results are in line with the observations in Figure 5 and further support a role of p58IPK in regulation of anti- and proapoptotic proteins in the Bcl-2 family.

Discussion

Protein p58IPK belongs to the DNAJ family and contains two types of protein interaction sites: a tetratricopeptide repeat (TPR) domain and a C-terminal J domain. Of the nine TPR motifs, TPR1–TPR3 are the binding sites with unfolded protein in ER lumen,[30] TRP6 motif is the site for inhibition of double-stranded RNA-dependent protein kinase (PKR) and PERK in cytosol,[10–12] while TRP7 is the binding site with p52rIPK, an inhibitor of p58IPK.[31] Therefore, p58IPK is a dual-function protein and its properties depend upon its location. Knockout of p58IPK results in upregulation of proapoptotic genes and pancreatic β-cell failure, suggesting that p58IPK is essential for β-cell survival.[28] In the present study, we used p58IPK KO mice to clarify the role of p58IPK in the retina. We showed that p58IPK is highly immunoreactive in retinal ganglion cells, ONL, and the inner segments of photoreceptors of WT mice. Knockout of p58IPK resulted in CHOP upregulation in ganglion cells and reduced cell number with aging, but did not alter the thicknesses of ONL and INL, indicating that p58IPK may play a more important role in RGCs than in other retinal neurons. Considered a key player in ER stress–mediated apoptosis,[32–34] CHOP is expressed at low levels under non-stressed conditions, but highly induced in response to ER stress.[35] Deletion of CHOP promotes ganglion cell survival in animal models of optic nerve injury,[26] which implicates CHOP and ER stress in ganglion cell death. Our findings from the p58IPK KO mice suggest that loss of p58IPK may render retinal ganglion cells more sensitive to ER stress, resulting in CHOP activation and ganglion cell degeneration. Additionally, deficiency of p58IPK—which is important for GRP78-mediated protein folding—could potentially affect RGC cell fate during retinal development by regulating the production of key factors involved in RGC differentiation, maturation, and remodeling. This speculation is supported by recent exciting studies that suggest an emerging role of ER chaperones such as GRP78 and signaling pathways of the UPR in the self-renewal, maturation, and differentiation of stem cells (reviewed in Zhang et al.[36]). Moreover, activation of the UPR signaling mediated by X-box binding protein 1 (XBP1), an upstream inducer of p58IPK, has been shown to be essential in neurite growth stimulated by brain-derived neurotrophic factor (BDNF).[37] Yet, the role of p58IPK and the underlying mechanisms in retinal neuronal development remain poorly understood and warrant a future investigation.

To further examine the role of p58IPK in retinal neuronal cell survival under stressed conditions, we employed the NMDA model, which has been widely used to investigate mechanisms of retinal neuronal cell death. Importantly, recent studies have demonstrated that intravitreal injection of NMDA induces a rapid increase of ER stress in retinal ganglion cells as early as 12 hours and that induction of ER stress by tunicamycin results in loss of ganglion cells and thinning of the inner plexiform layer 7 days after intravitreal injection.[38] These findings suggest ER stress plays a critical role in NMDA-induced ganglion cell death. Furthermore, pharmacological inhibition of PKR significant ameliorates ganglion cell loss in the NMDA model and reduced CHOP expression, suggesting PKR activation is also involved in NMDA-induced ganglion cell

Investigative Ophthalmology & Visual Science

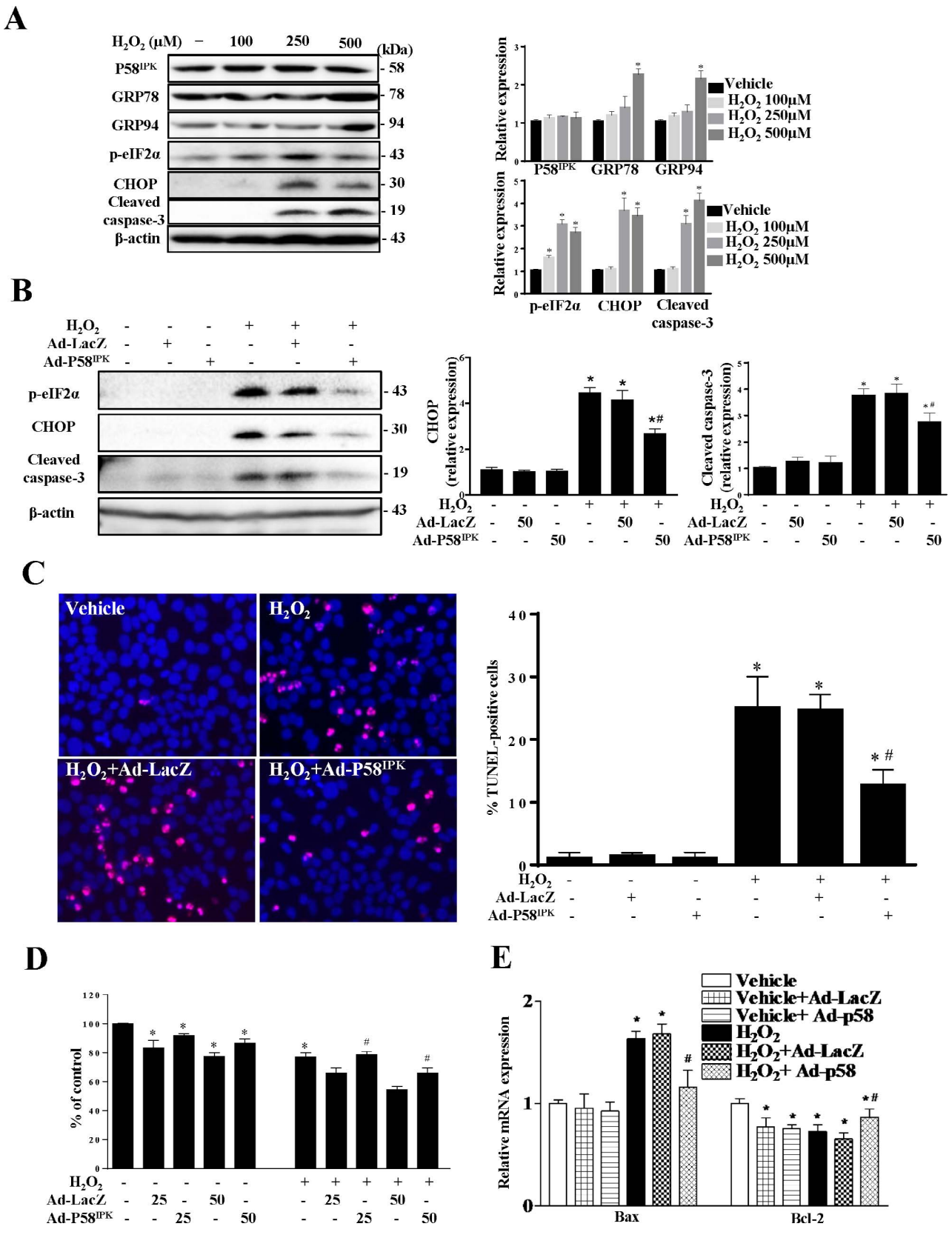

Figure 6. Overexpression of p58IPK attenuates ROS-induced ER stress and apoptosis. (**A**) R28 cells were treated with H_2O_2 for 24 hours. *Left panel*: Immunoblots showing increased expression of GRP78 and CHOP, phosphorylation of eIF2α and activation of caspase-3 by H_2O_2 in a dose-dependent manner. *Right panels*: The protein expression was semiquantified by densitometry (mean ± SD, $n = 4$). *$P < 0.01$ versus vehicle. (**B**) R28 cells were transduced with Ad-p58IPK and Ad-LacZ for 24 hours, followed by treatment with 500 μM H_2O_2 for 8 hours. *Left panel*: Immunoblotting demonstrating that overexpression of p58IPK decreases expression of CHOP, phosphorylation of eIF2α and activation of caspase-3 in H_2O_2-treated cells. *Right panels*: quantification of protein expression by densitometry (mean ± SD, $n = 4$). *$P < 0.001$ versus vehicle. #$P < 0.01$

versus Ad-LacZ + H_2O_2. (**C**) *Left panels*: Representative images of TUNEL staining in adenoviral transduced cells after treatment with 500 μM H_2O_2 for 8 hours. *Right panel*: quantification of TUNEL-positive cells. Results are means ± SD of 6 to 9 frames/group from four independent experiments. *$P < 0.001$ versus vehicle. #$P < 0.01$ versus Ad-LacZ + H_2O_2. (**D**) Cell viability measured by MTT assay in cells after H_2O_2 treatment for 8 hours. Results are means ± SD of four independent experiments. *$P < 0.001$ versus vehicle. #$P < 0.05$ versus corresponding Ad-LacZ + H_2O_2 group. (**E**) Results of qRT-PCR showing relative gene expression levels for Bax and Bcl-2. Results are mean ± SD of four independent experiments. *$P < 0.01$ versus vehicle. #$P < 0.05$ versus Ad-LacZ + H_2O_2.

death.[39] In our study, we showed that retinal ganglion cells in p58IPK-KO mice were less resistant to NMDA treatment resulting in more neuronal cell death compared with WT mice. This suggests that p58IPK, which acts as both an ER chaperone and an inhibitor of PKR, may function as an important protective factor in retinal ganglion cells.

Our in vitro study using immortalized R28 cells, derived from postnatal rat retinal cells, provided direct evidence of the protective effect of p58IPK in retinal neuronal cells. These cells are considered a retinal neural precursor cell line and display both glial and neuronal cell markers.[40,41] However, after maturation, R28 cells adopt a neuronal morphology and lose glial markers.[24] Since p58IPK is considered a dual functional protein and its property depends on its location, we performed immunostaining to examine the subcellular localization of p58IPK in R28 cells. We found that p58IPK mainly colocalized with ER-resident chaperones in the ER lumen. However, in control cells without tunicamycin treatment and/or after viral transduction by Ad-LacZ, a small portion of cytosolic p58IPK was also present. After induction of ER stress, p58IPK was primarily localized in the ER lumen. This observation is consistent with previous observations that p58IPK may localize in the cytosol of unstressed cells, but translocate into the ER upon ER stress by its N-terminal ER-targeting domain.[3]

In agreement with these results, we showed that overexpression of p58IPK protected R28 cells from ER stress. Our data suggest that mature R28 cells are sensitive to ER stress. At relative low doses (0.1–5.0 μg/mL), tunicamycin induced a dose-dependent increase in ER stress and expression of the apoptotic mediator cleaved caspase-3. In adenoviral-transduced cells, tunicamycin also resulted in PARP cleavage, another hallmark event of apoptosis, leading to apoptosis and cell death. Overexpression of p58IPK attenuated ER stress induced by tunicamycin, reduced apoptosis, and enhanced cell viability. In line with these results, previous studies have shown that overexpression of p58IPK inhibits ER stress in retinal endothelial cells and diabetic retinopathy.[42,43] These findings suggest that p58IPK has protective effects on retinal cells against ER stress.

Apart from ER stress, we demonstrated that p58IPK also protected R28 cells from oxidative stress–induced apoptotic cell death. Previous studies have shown that ER stress and oxidative stress are closely inter-related and have the potential to cause a vicious cycle of damage.[44] Specifically, the ER lumen has a highly oxidizing environment due to the protein folding process, a highly energy-dependent process that generates reactive oxidative species (ROS) as a by-product.[45] In addition, the recycling process of the folding enzyme protein disulfide isomerase involves the thiol oxidase Ero1. Moreover, oxidative stress due to increased ROS acts as an intracellular signal that can cause calcium influx into the cytoplasm and the ER. Disturbance of calcium balance and alteration of the ER's oxidative environment can negatively impact protein folding, resulting in ER stress and ROS generation.[45] One ROS, hydrogen peroxide, plays a role in intracellular signal transduction.[46] Excess exogenous hydrogen peroxide can induce oxidative stress by increasing intracellular ROS accumulation. Oxidative stress induced by treatment with hydrogen peroxide causes apoptosis by either caspase-independent[47] or -dependent pathways.[48] In the present study, we showed that hydrogen peroxide induced oxidative stress and caused apoptosis by a caspase-dependent pathway in R28 cells. Hydrogen peroxide increased expression of chaperones, CHOP and p-eIF2α in a dose-dependent manner, indicating an induction of ER stress. Overexpression of p58IPK alleviated ER stress, reduced apoptosis and increased viability of R28 cells, suggesting a protective effect of p58IPK against oxidative stress-induced neuronal injury.

Finally, our data indicated that p58IPK may exert its protective effects through regulating Bcl-2 family proteins. The Bcl-2 family consists of antiapoptotic members, such as Bcl-2 and Bcl-xL, and proapoptotic proteins, such as Bax, Bak, and Bik, which are considered the central co-ordinators of mitochondria-mediated apoptotic pathways.[49] Studies have shown that both the anti-apoptotic gene Bcl-2 and the proapoptotic gene Bax are regulated by CHOP during ER stress.[50] An important transcription factor, XBP1, regulates the adaptive UPR and induces ER chaperones including p58IPK. Our recent work showed that deletion of XBP1 in RPE cells resulted in decreased Bcl-2 but increased CHOP expression and apoptosis, while overexpression of XBP1 protected the RPE from oxidative damage.[25] This observation, in good agreement with the results from the current study, supports the notion that XBP1 and its downstream ER chaperone genes are vital for retinal cell survival, possibly by regulating the ER homeostasis and suppressing mitochondria-related apoptotic pathways.

Acknowledgments

We thank Michael Katze, PhD (University of Washington, Seattle, WA, USA) for providing P58IPK knockout mice.

Presented in part at the annual meeting of the Association for Research in Vision and Ophthalmology, Orlando, Florida, United States, May 2014.

Supported, in part, by NIH/NEI Grants EY019949 and EY025061, a grant from the American Diabetes Association, and an unrestricted grant to the Department of Ophthalmology, SUNY-Buffalo, from Research to Prevent Blindness (SXZ).

Disclosure: **E. Boriushkin**, None; **J.J. Wang**, None; **J. Li**, None; **G. Jing**, None; **G.M. Seigel**, KeraFAST, Inc. (C); **S.X. Zhang**, None

References

1. Xu C, Bailly-Maitre B, Reed JC. Endoplasmic reticulum stress: cell life and death decisions. *J Clin Invest*. 2005;115:2656–2664.
2. Ron D, Walter P. Signal integration in the endoplasmic reticulum unfolded protein response. *Nat Rev Cell Biol*. 2007;8:519–529.
3. Rutkowski DT, Kang SW, Goodman AG, et al. The role of p58IPK in protecting the stressed endoplasmic reticulum. *Mol Biol Cell*. 2007;18:3681–3691.
4. Tao J, Wu Y, Ron D, Sha B. Preliminary x-ray crystallographic studies of mouse UPR responsive protein P58(IPK) TPR fragment. *Acta Crystallogr Sect F Struct Biol Cryst Commun*. 2008;64:108–110.

5. Tao J, Sha B. Structural insight into the protective role of P58(IPK) during unfolded protein response. *Methods Enzymol*. 2011;490:259–270.
6. Petrova K, Oyadomari S, Hendershot LM, Ron D. Regulated association of misfolded endoplasmic reticulum lumenal proteins with P58/DNAJc3. *EMBO J*. 2008;27:2862–2872.
7. Flynn GC, Pohl J, Flocco MT, Rothman JE. Peptide-binding specificity of the molecular chaperone BiP. *Nature*. 1991;353:726–730.
8. Gething MJ. Role and regulation of the ER chaperone BiP. *Semin Cell Dev Biol*. 1999;10:465–472.
9. Chakrabarti A, Chen AW, Varner JD. A review of the mammalian unfolded protein response. *Biotechnol Bioeng*. 2011;108:2777–2793.
10. Melville MW, Hansen WJ, Freeman BC, Welch WJ, Katze MG. The molecular chaperone hsp40 regulates the activity of P58IPK, the cellular inhibitor of PKR. *Proc Natl Acad Sci U S A*. 1997;94:97–102.
11. Polyak SJ, Tang N, Wambach M, Barber GN, Katze MG. The P58 cellular inhibitor complexes with the interferon-induced, double-stranded RNA-dependent protein kinase, PKR, to regulate its autophosphorylation and activity. *J Biol Chem*. 1996;271:1702–1707.
12. Tang NM, Ho CY, Katze MG. The 58-kDA cellular inhibitor of the double stranded RNA-dependent protein kinase requires the tetratricopeptide repeat 6 and Dnaj motifs to stimulate protein synthesis in vivo. *J Biol Chem*. 1996;271:28660–28666.
13. Doh SH, Kim JH, Lee KM, Park HY, Park CK. Retinal ganglion cell death induced by endoplasmic reticulum stress in a chronic glaucoma model. *Brain Res*. 2010;1308:158–166.
14. Aoki S, Su Q, Li H, et al. Identification of an axotomy-induced glycosylated protein, AIGP1, possibly involved in cell death triggered by endoplasmic reticulum-Golgi stress. *J Neurosci*. 2002;22:10751–10760.
15. Oshitari T, Hata N, Yamamoto S. Endoplasmic reticulum stress and diabetic retinopathy. *Vasc Health Risk Manag*. 2008;4:115–122.
16. McKinnon SJ. Glaucoma, apoptosis, and neuroprotection. *Curr Opin Ophthalmol*. 1997;8:28–37.
17. Bonne C, Muller A, Villain M. Free radicals in retinal ischemia. *Gen Pharmacol*. 1998;30:275–280.
18. Sattler R, Tymianski M. Molecular mechanisms of glutamate receptor-mediated excitotoxic neuronal cell death. *Mol Neurobiol*. 2001;24:107–129.
19. Hajnoczky G, Davies E, Madesh M. Calcium signaling and apoptosis. *Biochem Biophys Res Commun*. 2003;304:445–454.
20. Paschen W, Frandsen A. Endoplasmic reticulum dysfunction–a common denominator for cell injury in acute and degenerative diseases of the brain? *J Neurochem*. 2001;79:719–725.
21. Awai M, Koga T, Inomata Y, et al. NMDA-induced retinal injury is mediated by an endoplasmic reticulum stress-related protein, CHOP/GADD153. *J Neurochem*. 2006;96:43–52.
22. Li J, Wang JJ, Zhang SX. Preconditioning with endoplasmic reticulum stress mitigates retinal endothelial inflammation via activation of X-box binding protein 1. *J Biol Chem*. 2011;286:4912–4921.
23. Seigel GM. Review: R28 retinal precursor cells: The first 20 years. *Mol Vis*. 2014;20:301–306.
24. Barber AJ, Nakamura M, Wolpert EB, et al. Insulin rescues retinal neurons from apoptosis by a phosphatidylinositol 3-kinase/Akt-mediated mechanism that reduces the activation of caspase-3. *J Biol Chem*. 2001;276:32814–32821.
25. Chen C, Cano M, Wang JJ, et al. Role of unfolded protein response dysregulation in oxidative injury of retinal pigment epithelial cells. *Antioxid Redox Signal* 2013;20:2091–2106.
26. Hu Y, Park KK, Yang L, et al. Differential effects of unfolded protein response pathways on axon injury-induced death of retinal ganglion cells. *Neuron*. 2012;73:445–452.
27. Ramirez JM, Trivino A, Ramirez AI, Salazar JJ, Garcia-Sanchez J. Immunohistochemical study of human retinal astroglia. *Vision Res*. 1994;34:1935–1946.
28. Ladiges WC, Knoblaugh SE, Morton JF, et al. Pancreatic beta-cell failure and diabetes in mice with a deletion mutation of the endoplasmic reticulum molecular chaperone gene P58IPK. *Diabetes*. 2005;54:1074–1081.
29. Joo CK, Choi JS, Ko HW, et al. Necrosis and apoptosis after retinal ischemia: Involvement of NMDA-mediated excitotoxicity and p53. *Invest Ophthalmol Vis Sci*. 1999;40:713–720.
30. Tao J, Petrova K, Ron D, Sha B. Crystal structure of p58(IPK) TPR fragment reveals the mechanism for its molecular chaperone activity in UPR. *J Mol Biol*. 2010;397:1307–1315.
31. Gale M Jr, Blakely CM, Hopkins DA, et al. Regulation of interferon-induced protein kinase PKR: modulation of P58IPK inhibitory function by a novel protein, P52rIPK. *Mol Cell Biol*. 1998;18:859–871.
32. Oyadomari S, Takeda K, Takiguchi M, et al. Nitric oxide-induced apoptosis in pancreatic beta cells is mediated by the endoplasmic reticulum stress pathway. *Proc Natl Acad Sci U S A*. 2001;98:10845–10850.
33. Oyadomari S, Koizumi A, Takeda K, et al. Targeted disruption of the chop gene delays endoplasmic reticulum stress-mediated diabetes. *J Clin Invest*. 2002;109:525–532.
34. Tsutsumi S, Gotoh T, Tomisato W, et al. Endoplasmic reticulum stress response is involved in nonsteroidal anti-inflammatory drug-induced apoptosis. *Cell Death Differ*. 2004;11:1009–1016.
35. Ron D, Habener JF. CHOP, a novel developmentally regulated nuclear protein that dimerizes with transcription factors C/EBP and LAP and functions as a dominant-negative inhibitor of gene transcription. *Genes Dev*. 1992;6:439–453.
36. Zhang SX, Ma JH, Bhatta M, Fliesler SJ, Wang JJ. The unfolded protein response in retinal vascular diseases: Implications and therapeutic potential beyond protein folding [published online ahead of print December 18, 2014]. *Prog Retin Eye Res*. doi:10.1016/j.preteyeres.2014.12.001.
37. Hayashi A, Kasahara T, Iwamoto K, et al. The role of brain-derived neurotrophic factor (BDNF)-induced XBP1 splicing during brain development. *J Biol Chem*. 2007;282:34525–34534.
38. Shimazawa M, Inokuchi Y, Ito Y, et al. Involvement of ER stress in retinal cell death. *Mol Vis*. 2007;13:578–587.
39. Shimazawa M, Ito Y, Inokuchi Y, Hara H. Involvement of double-stranded RNA-dependent protein kinase in ER stress-induced retinal neuron damage. *Invest Ophthalmol Vis Sci*. 2007;48:3729–3736.
40. Seigel GM, Mutchler AL, Imperato EL. Expression of glial markers in a retinal precursor cell line. *Mol Vis*. 1996;2:2.
41. Seigel GM, Sun W, Wang J, Hershberger DH, Campbell LM, Salvi RJ. Neuronal gene expression and function in the growth-stimulated R28 retinal precursor cell line. *Curr Eye Res*. 2004;28:257–269.
42. Li B, Li D, Li GG, Wang HW, Yu AX. P58(IPK) inhibition of endoplasmic reticulum stress in human retinal capillary endothelial cells in vitro. *Mol Vis*. 2008;14:1122–1128.
43. Yang H, Liu R, Cui Z, et al. Functional characterization of 58-kilodalton inhibitor of protein kinase in protecting against diabetic retinopathy via the endoplasmic reticulum stress pathway. *Mol Vis*. 2011;17:78–84.
44. Hwang C, Sinskey AJ, Lodish HF. Oxidized redox state of glutathione in the endoplasmic reticulum. *Science*. 1992;257:1496–1502.

Investigative Ophthalmology & Visual Science

45. Malhotra JD, Kaufman RJ. Endoplasmic reticulum stress and oxidative stress: a vicious cycle or a double-edged sword? *Antioxid Redox*. 2007;9:2277–2293.
46. Veal EA, Day AM, Morgan BA. Hydrogen peroxide sensing and signaling. *Mol Cell* 2007;26:1–14.
47. Li GY, Osborne NN. Oxidative-induced apoptosis to an immortalized ganglion cell line is caspase independent but involves the activation of poly(ADP-ribose)polymerase and apoptosis-inducing factor. *Brain Res*. 2008;1188:35–43.
48. Cheng XR, Zhang L, Hu JJ, Sun L, Du GH. Neuroprotective effects of tetramethylpyrazine on hydrogen peroxide-induced apoptosis in PC12 cells. *Cell Biol Int*. 2007;31:438–443.
49. Jing G, Wang JJ, Zhang SX. ER stress and apoptosis: a new mechanism for retinal cell death. *Exp Diabetes Res*. 2012; 2012:589589.
50. Szegezdi E, Logue SE, Gorman AM, Samali A. Mediators of endoplasmic reticulum stress-induced apoptosis. *EMBO Rep*. 2006;7:880–885.

Investigative Ophthalmology & Visual Science